materials

MDPI

Article

# Enhanced Visible Transmittance of Thermochromic $VO_2$ Thin Films by $SiO_2$ Passivation Layer and Their Optical Characterization

**Jung-Hoon Yu [1], Sang-Hun Nam [2], Ji Won Lee [1,2] and Jin-Hyo Boo [1,2,*]**

[1] Department of Chemistry, Sungkyunkwan University, Suwon 440-746, Korea; thank42@hanmail.net (J.-H.Y.); ljw9917@naver.com (J.W.L.)

[2] Institute of Basic Science, Sungkyunkwan University, Suwon 440-746, Korea; askaever@gmail.com

* Correspondence: jhboo@skku.edu; Tel.: +82-31-290-5972

Academic Editor: Shoou-Jinn Chang

Received: 29 May 2016; Accepted: 29 June 2016; Published: 9 July 2016

**Abstract:** This paper presents the preparation of high-quality vanadium dioxide ($VO_2$) thermochromic thin films with enhanced visible transmittance ($T_{vis}$) via radio frequency (RF) sputtering and plasma enhanced chemical vapor deposition (PECVD). $VO_2$ thin films with high $T_{vis}$ and excellent optical switching efficiency ($E_{os}$) were successfully prepared by employing $SiO_2$ as a passivation layer. After $SiO_2$ deposition, the roughness of the films was decreased 2-fold and a denser structure was formed. These morphological changes corresponded to the results of optical characterization including the haze, reflectance and absorption spectra. In spite of $SiO_2$ coating, the phase transition temperature ($T_c$) of the prepared films was not affected. Compared with pristine $VO_2$, the total layer thickness after $SiO_2$ coating was 160 nm, which is an increase of 80 nm. Despite the thickness change, the $VO_2$ thin films showed a higher $T_{vis}$ value (λ 650 nm, 58%) compared with the pristine samples (λ 650 nm, 43%). This enhancement of $T_{vis}$ while maintaining high $E_{os}$ is meaningful for $VO_2$-based smart window applications.

**Keywords:** $VO_2$; thermochromic; $SiO_2$ passivation

## 1. Introduction

For improved design and practicality, the exterior of many buildings has been changed into full-window constructions in recent years [1]. However, such window architecture systems lead to more cooling and heating energy loss in the summer and winter seasons. One of the best ways to solve this problem is vanadium dioxide ($VO_2$) based thermochromic smart windows. $VO_2$ is a well-known material that undergoes a fully reversible metal-insulator phase transition (MIT) at 68 °C accompanied by structural changes from a monoclinic (semiconductor with high IR transparency) to a rutile (metallic form with IR reflection) phase [2,3]. These unique properties make $VO_2$ a promising material for application in energy saving smart windows with solar heat control [4–8]. However, for practical applications, several challenges must be improved: the transition temperature ($T_c$) is too high to apply on real field; the weak optical contrast in the IR region; the luminous transmittance ($T_{lum}$) is less than ~40% for films; the unfavorable color (yellow/brown). Up to now, there have been many efforts to improve the above issues [9,10]. More than anything, low visible transmittance ($T_{vis}$) is the most critical drawback of $VO_2$ for applications in glazing systems. The low $T_{vis}$ originates from strong innerband and interband absorption in the short-wavelength range for both the metallic and semiconductive states [11,12]. To enhance the $T_{vis}$, band gap adjustment by doping has been attempted. Zhou et al. reported on the preparation of Mg-doped $VO_2$ nanoparticles via hydrothermal synthesis [13]. By controlling the Mg doping contents, they demonstrated the absorption edge of $VO_2$

particles with a blue-shift from 490 to 440 nm at a Mg content of 3.8 at %, representing a widened optical band gap from 2.0 eV for pure $VO_2$ to 2.4 eV with 3.8 at % doping. Similar research was reported by Chen et al., who fabricated Ti-doped $VO_2$ nanoparticles with successful improvement of $T_{vis}$ by up to 53% via a hydrothermal process [14]. Zhou et al. reported another approach to improve the $T_{vis}$ of $VO_2$ thin films by designing $VO_2$ thin films with a periodic porous structure [15]. These periodic porous thermochromic $VO_2$ thin films were fabricated via a colloidal lithography approach and exhibited a high $T_{vis}$ (81% maximum). However, in spite of the significant enhancement of the $T_{vis}$, the optical switching efficiency ($E_{os}$) of previously reported $VO_2$ thin films is still lower that of traditional low-emission glass. Moreover, it is difficult to control the stoichiometry of a vanadium-oxygen system using the colloidal lithography approach because organic residues from the colloid might influence the valence of $VO_2$ as well as the phase transformation during the annealing process. $VO_2$-based multi-layered structures such as $VO_2/ZrO_2$ double layers [16] and $TiO_2/VO_2/TiO_2$ triple layers [17] are the most effective solutions to the above problems. These antireflective layers including $ZrO_2$ and $TiO_2$ can protect $VO_2$ from oxidation and provide new functions such as photocatalysis in addition to improving the visible transmittance. However, to date, the reported results on applying an anti-reflective layer have been based on more complex procedures or solution processes for which additional annealing is essential. Thus, the reported $VO_2$ thin films contain low $E_{os}$ originating from inconsistent stoichiometry due to additional annealing or other procedures [18,19].

In this work, high-quality $VO_2$ thermochromic thin films with significantly enhanced $T_{vis}$ were prepared by applying a $SiO_2$ layer using plasma enhanced chemical vapor deposition (PECVD). This $SiO_2$ layer deposited by the PECVD method has advantages such as the lack of additional post-annealing processes. Thus, damages from oxidation or reduction, which can influence the crystallinity of $VO_2$, do not occur during $SiO_2$ deposition. In addition, high uniformity and reproducibility underscore the attractiveness of PECVD. This paper also explains how the improvement of $T_{vis}$ was identified through optical analysis.

## 2. Materials and Methods

### *2.1. $SiO_2/VO_2$ Thin Film Preparation*

$VO_2$ thin films were prepared by RF magnetron sputtering with $VO_2$ ceramic targets (Taewon Scientific, Seoul, Korea, 99.9%, 2 inch). Before deposition, the Eagle XG glass (Corning, New York, NY, USA, 2.5 × 2.5 $cm^2$) used as a substrate was cleaned ultrasonically with hydrochloric acid (1 M) and Ethanol, then was subsequently dried with $N_2$. The vacuum chamber was evacuated to $1.2 \times 10^{-5}$ Torr, and Ar gas was introduced with 150 sccm. The RF power, working pressure, and distance of the target to the substrate were maintained at 180 W, 46 mTorr and 40 mm, respectively. The deposition time for all samples was fixed at 15 min. The prepared $VO_x$ thin films were crystallized via post-annealing under vacuum conditions (10 mTorr) at a temperature of 575 °C for 4 h with a heating rate of 30 °C/min. The $SiO_2$ layer was deposited by PECVD onto the as prepared $VO_2$ thin films under a working pressure of 200 mTorr. Hexamethyldisilazane (HMDSN) was used as a precursor and a thickness of 80 nm was achieved for the $SiO_2$. More detail procedure and conditions of PECVD is described elsewhere [20].

### *2.2. Characterizations*

The surface morphologies of the films were determined using FE-SEM (JEOL, JSM-7100 F, Tokyo, Japan) and AFM (PARK system, XE-100, Suwon, Korea). Crystallization information for the films was determined using X-ray diffraction (XRD) (Bruker D8 Advance system, Billerica, MA, USA) with Cu K$\alpha$ radiation ($\lambda$ = 1.5416 Å). Diffraction patterns were collected for 2$\theta$ values between 10° and 80° with a 2° glancing angle, and scanned at a rate of 5°/min. The phases present were identified by comparing the peak intensities and their corresponding 2$\theta$ values to various vanadium oxide standards using the software PCPDFWIN ver. 2.1 (JCPDS-ICDD, Philadelphia, PA, USA). Raman spectra were collected with a confocal Raman microscope (Witec, ALPHA 300 M, Ulm, Germany) based on the 532 nm $CO_2$

laser. The optical and thermochromic properties of the films were measured at the temperature range between 20 to 100 °C by using a UV-vis-NIR spectrometer (SHIMADZU, UV-3600, Kyoto, Japan) equipped with handmade heating units including a PID temperature controller. For all samples, the integral visible transmittance ($T_{lum}$, 390–830 nm) and solar transmittance ($T_{sol}$, 280–2500 nm) was obtained based on the earlier publication [21].

## 3. Results and Discussion

Figure 1 shows the SEM and AFM images of surface morphologies for the pristine $VO_2$ and $SiO_2/VO_2$ thin films. For the pristine $VO_2$, the mean grain size and film thickness were around 150 nm and 80 nm, respectively. Moreover, the clearly formed grain boundary was attributed to the surface roughness value of 11.87 nm. On the other hand, changes in the surface morphology of the films with denser and smoother grain boundaries, including those with 160 nm of total thickness, were observed after $SiO_2$ coating. In addition, an average roughness value of 4.91 nm was obtained, which is a 2-fold decrease compared to pristine $VO_2$. The obtained results suggest that the empty space between the grain boundary of pristine $VO_2$ was filled with $SiO_2$ during the PECVD process.

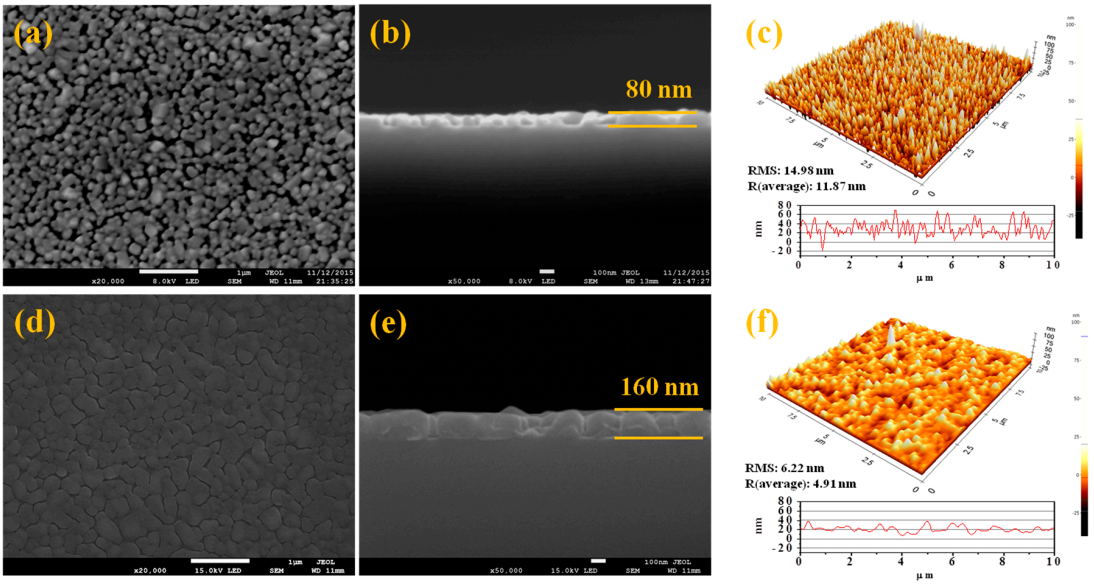


**Figure 1.** SEM and AFM images of $VO_2$ (**a**–**c**) and $SiO_2/VO_2$ (**d**–**f**) thin films. The average roughness of the samples was (**c**): 11.87 nm and (**f**): 4.91 nm.

Figure 2 shows the XRD data and Raman spectra for each sample. The XRD pattern showed weak signal intensities for the crystallite, resulting from the short-range ordered nanocrystallinity and thinness of the films. The broad shoulder within 15°–40° is due to the contribution of the amorphous $SiO_2$ substrate [22]. A peak at 27.8° that can be ascribed to the (011) plane of monoclinic $VO_2$ (JCPDS no. 82-0661) was observed in the pristine $VO_2$ thin films. For the $SiO_2/VO_2$ thin films however, decreased peak intensity was observed, originating from disruption of the thickly covered $SiO_2$ film. Most importantly, no clear diffraction peaks for other vanadium oxides were observed. Raman models corresponding to $VO_2$ (M) appeared in each sample with peaks centered at 135, 192, 225, 263, 308, 338, 392, 440, 499, and 617 $cm^{-1}$ [23]. The change in Raman shifts for the films was within the measurement accuracy ($\pm 2$ $cm^{-1}$). For pristine $VO_2$ thin film, peaks from other types of vanadium oxide were not observed. Moreover, the peaks around 195 $cm^{-1}$ and 225 $cm^{-1}$ corresponded to $A_g$ symmetry vibrational modes, which disappeared in $VO_2$ (R) [24,25]. These two vibrational modes play a decisive role in the structural transition of $VO_2$. Thus, the appearance of strong peaks suggests high optical switching characteristics. After $SiO_2$ coating, however, a broad peak around 480 $cm^{-1}$ attributed to amorphous $SiO_2$ was observed with a moderate signal to noise ratio while the initial

peaks corresponding to $VO_2$ (M) remained. In other words, $SiO_2$ coating via PECVD does not affect the crystallinity of $VO_2$ thin films. The corresponding evidence is shown in Figure 3b,c. The hysteresis loop at 2000 nm was obtained from the optical transmittance of each sample as a function of temperature, and a plot of d(Tr)/d(T)&T was obtained from one peak with a well-defined maximum. Each of the d(Tr)/d(T)&T curves were analyzed with a Gaussian function using the single peak fitting module in Origin pro 8.0 software (Originlab, Washington, DC, USA). Distinguishable changes in $T_c$ and hysteresis width, which are closely related to the crystallographic orientation [26], were not observed except for a slight decrease in transmittance.

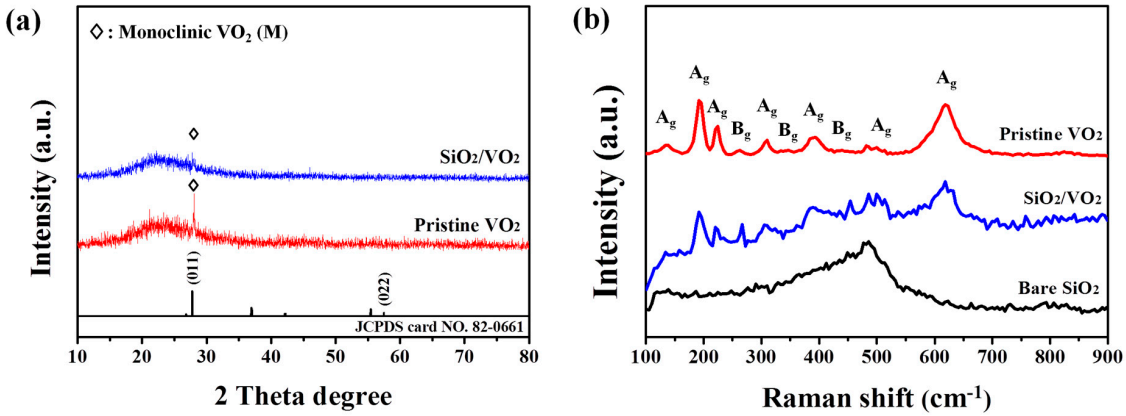


**Figure 2.** X-ray diffraction (XRD) (**a**) and Raman spectra (**b**) of $VO_2$ and $SiO_2/VO_2$ thin films.

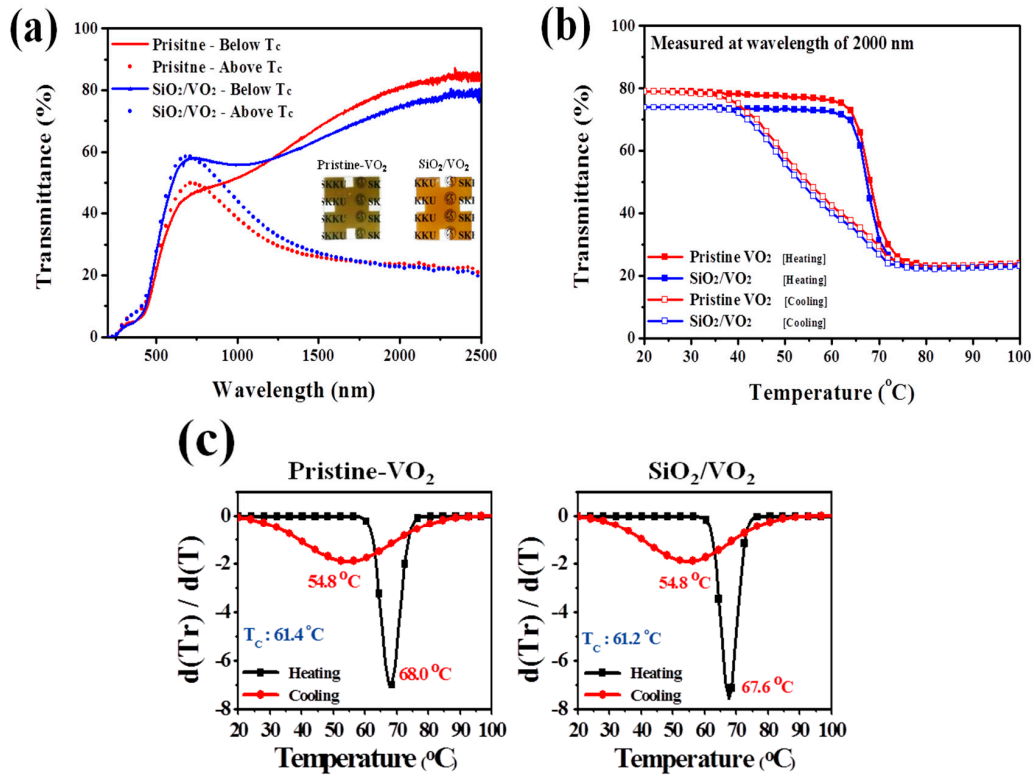


**Figure 3.** Transmittance spectra (**a**); hysteresis loops at 2000 nm (**b**) as well as corresponding d(Tr)/d(T)&T curve (**c**) for pristine $VO_2$ and $SiO_2/VO_2$ thin films. The inset images in (**a**) correspond respectively to photographs of the pristine $VO_2$ film (left) and $VO_2/SiO_2$ film (right). In (**a**), solid line measured at 25 °C, dashed line at 100 °C.

The optical analysis results for each sample are shown in Figure 3a. Transmittance results demonstrate the thermochromic properties of each sample measured at 20 °C (solid line) and 100 °C (dashed line). The $E_{os}$ of the $SiO_2/VO_2$ films was 51.7%, which is slightly lower compared with pristine $VO_2$ thin films (57.1%), but the difference is not significant. The $SiO_2/VO_2$ thin films showed a significantly enhanced $T_{vis}$ value ($\lambda_{650\ nm}$, 58%) compared with the pristine samples ($\lambda_{650\ nm}$, 43%). In addition, the inset images in Figure 3a clearly show a contrast change after $SiO_2$ coating. Though the $SiO_2/VO_2$ film is thicker, it exhibited higher $T_{vis}$ than the pristine $VO_2$. This enhancement of $T_{vis}$ can be attributed to two factors. Furthermore, these optical results can be defined by average $T_{lum}((T_{lum,\ 20\ °C} + T_{lum,\ 100\ °C})/2)$ and $\Delta T_{sol}(T_{sol,\ 20\ °C} - T_{sol,\ 100\ °C})$. The average $T_{lum}$ of pristine and $SiO_2/VO_2$ films are 37.6% and 47.7%, respectively, and $\Delta T_{sol}$ are 8.06 and 7.62. One is the difference in reflectance between pristine $VO_2$ and $SiO_2/VO_2$ thin films in the visible region as shown in Figure 4a. As previously mentioned, the formation of smoother and denser grain boundaries after $SiO_2$ coating could reduce the surface roughness, which can influence the decrease of light scattering on the surface observed in SEM images. Therefore, the reflectance for the $SiO_2/VO_2$ thin films was decreased from 8% to 4% compared to the pristine $VO_2$ thin films. However, the change in the reflectance is not enough to confirm the enhancement of $T_{vis}$ for $SiO_2/VO_2$ thin films. Figure 4b shows the haze for each sample in the visible region. For the $SiO_2/VO_2$ thin films, a slight decrease in haze over 500 nm was observed but other considerable changes did not appear. For this reason, more evidence is needed to validate the transmittance results.

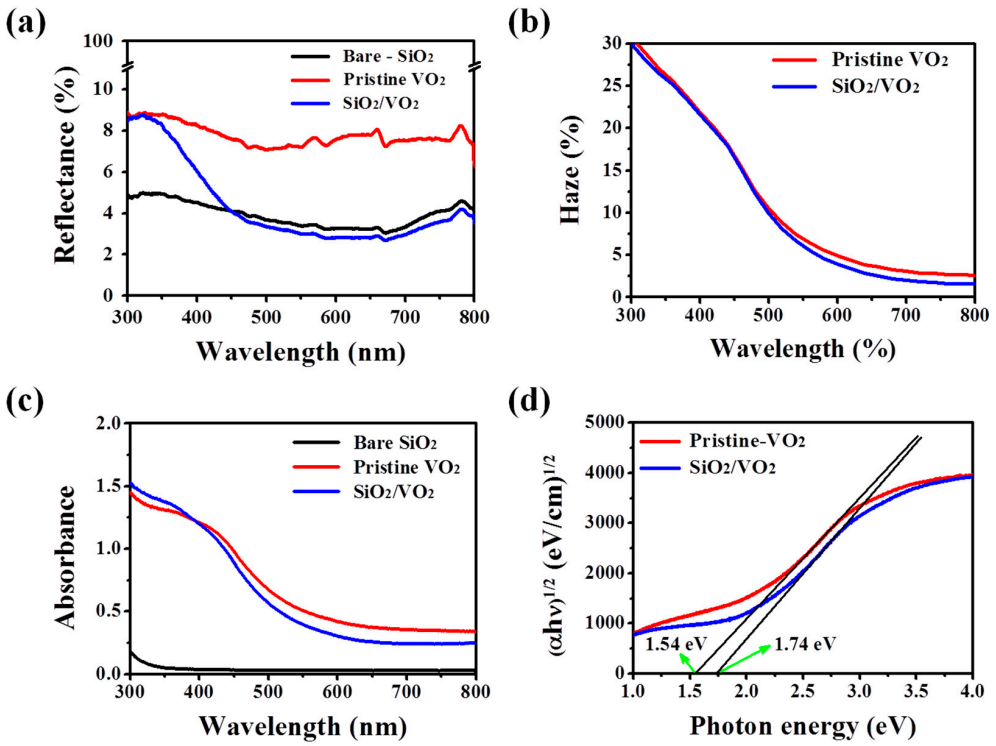


**Figure 4.** Optical analysis data for each film based on the reflectance (**a**); haze (**b**); absorbance (**c**) and optical band gap graph (**d**).

Figure 4c shows the absorbance data for each sample measured in the visible region. The data obviously confirm the change in the absorption edge toward the blue region and a decrease in absorbance after $SiO_2$ coating. The relative optical band gap for each sample is shown in Figure 4d, and the results correspond to the results for reflectance and absorbance. The absorption coefficient $\alpha$ was estimated using the transmittance data for the two films [27].

$$\alpha = (1/\Delta d)\ln(T_1/T_2) \quad (1)$$

where $\Delta d$ is the thickness of pristine $VO_2$ or $SiO_2/VO_2$, $T_1$ is the transmittance of the substrate (Eagle glass) and $T_2$ is the transmittance of each sample. The optical band gap was determined with the following formula [28].

$$(\alpha h\nu)^{1/2} \propto (E - E_g) \quad (2)$$

linear extrapolation of $(\alpha h\nu)^{1/2}$ vs. $h\nu$ near the band gap provided $E_g$ as the intercept at the $\alpha = 0$ axis. The optical band gap for the pristine $VO_2$ thin film increased from 1.54 to 1.74 eV after $SiO_2$ coating. This widening of the optical band gap induces a blue shift and an enhanced visible transmittance [15]. This means that the enhancement of $T_{vis}$ for $SiO_2/VO_2$ corresponds to the decrease in absorbance and reflectance including the formation of denser and smoother surfaces on the films.

## 4. Conclusions

In this paper, high-quality $VO_2$ thermochromic thin films with enhanced $T_{vis}$ up to 58% were successfully prepared with the addition of a $SiO_2$ layer. The results indicate that the enhanced $T_{vis}$ was due to a reduction of surface roughness with a blue shift in the absorption spectra observed after $SiO_2$ coating. In addition, the $SiO_2/VO_2$ thin films had high $E_{os}$ and the crystallographic orientation was maintained. This enhancement of $T_{vis}$ while maintaining high $E_{os}$ is meaningful for $VO_2$-based smart window applications.

**Acknowledgments:** This work was supported by the Mid-career Researcher Program (2015R1A2A2A01007150) through an National Research Foundation of Korea (NRF) grant funded by the Ministry of Education, Science and Technology (MEST) and the Energy Efficiency & Resources Core Technology Program of the Korea Institute of Energy Technology Evaluation and Planning (KETEP), granted financial resource from the Ministry of Trade, Industry & Energy, Republic of Korea. (No. 20142020104130).

**Author Contributions:** Sang-Hun Nam and Jin-Hyo Boo proposed the research topic and supervised the entire project. Jung-Hoon Yu designed the experiments, performed the optical characterization and wrote the manuscript. All the authors contributed to the writing and approved the final manuscript.

**Conflicts of Interest:** The authors declare no conflict of interest.

## Abbreviations

The following abbreviations are used in this manuscript:

| | |
|---|---|
| PECVD | Plasma enhanced chemical vapor deposition |
| $T_{vis}$ | Visible transmittance |
| $E_{os}$ | Optical switching efficiency |
| $VO_2$ | Vanadium dioxide |
| MIT | Metal-insulator transition |
| SEM | Scanning electron microscopy |
| XRD | X-ray diffraction |

## References

1. Hee, W.J.; Alghoul, M.A.; Bakhtyar, B.; OmKalthum, E.; Shameri, M.A.; Alrubaih, M.S.; Sopian, K. The role of window glazing on daylighting and energy saving in buildings. *Renew. Sustain. Energy Rev.* **2015**, *42*, 323–343. [CrossRef]
2. Morin, F.J. Oxides which show a metal-to-insulator transition at the neel temperature. *Phys. Rev. Lett.* **1959**, *3*, 34–36. [CrossRef]
3. Qazilbash, M.M.; Brehm, M.; Andreev, G.O.; Kim, B.J.; Yun, S.J.; Balatsky, A.V.; Maple, M.B.; Keilmann, F.; Kim, H.T.; Basov, D.N. Mott transition in $VO_2$ revealed by infrared spectroscopy and nano-imaging. *Science* **2007**, *318*, 1750–1753. [CrossRef] [PubMed]
4. Cao, C.; Gao, Y.; Luo, H. Pure single-crystal rutile vanadium dioxide powders: Synthesis, mechanism and phase-transformation property. *J. Phys. Chem. C* **2008**, *112*, 18810–18814. [CrossRef]

5. Kang, L.; Gao, Y.; Luo, H. A Novel solution process for the synthesis of $VO_2$ thin films with excellent thermochromic properties. *ACS Appl. Mater. Interfaces* **2009**, *1*, 2211–2218. [CrossRef] [PubMed]
6. Mlyuka, N.R.; Niklasson, G.A.; Granqvist, C.G. Thermochromic multilayer films of $VO_2$ and $TiO_2$ with enhanced transmittance. *Sol. Energy Mater. Sol. Cells* **2009**, *93*, 1685–1687. [CrossRef]
7. Vernardou, D.; Louloudakis, D.; Spanakis, E.; Katsarakis, N.; Koudoumas, E. Thermochromic amorphous $VO_2$ coatings grown by APCVD using a single-precursor. *Sol. Energy Mater. Sol. Cells* **2014**, *128*, 36–40. [CrossRef]
8. Drosos, C.; Vernardou, D. Perspectives of energy materials grown by APCVD. *Sol. Energy Mater. Sol. Cells* **2015**, *140*, 1–8. [CrossRef]
9. Wang, S.; Liu, M.; Kong, L.; Long, Y.; Jiang, X.; Yu, A. Recent progress in $VO_2$ smart coating: Strategies to improve the thermochromic properties. *Prog. Mater. Sci.* **2016**, *81*, 1–54. [CrossRef]
10. Zhou, Y.; Cai, Y.; Hu, X.; Long, Y. $VO_2$/hydrogel hybrid nanothermochromic material with ultra-high solar modulation and luminous transmission. *J. Mater. Chem. A* **2015**, *3*, 1121–1126. [CrossRef]
11. Burkhardt, W.; Christmann, T.; Franke, S.; Kriegseis, W.; Meister, D.; Meyer, B.K.; Niessner, W.; Schalch, D.; Scharmann, A. Tungsten and fluorine co-doping of $VO_2$ films. *Thin Sol. Films* **2002**, *402*, 226–231. [CrossRef]
12. Qazilbash, M.M.; Schafgans, A.A.; Burch, K.S.; Yun, S.J.; Chae, B.G.; Kim, B.J.; Kim, H.T.; Basov, D.N. Electrodynamics of the vanadium oxides $VO_2$ and $V_2O_3$. *Phys. Rev. B* **2008**, *77*, 115121. [CrossRef]
13. Zhou, J.; Gao, Y.; Liu, X.; Chen, Z.; Dai, L.; Cao, C.; Luo, H.; Kanahira, M.; Sunc, C.; Yanc, L. Mg-doped $VO_2$ nanoparticles: Hydrothermal synthesis, enhanced visible transmittance and decreased metal–insulator transition temperature. *Phys. Chem. Chem. Phys.* **2013**, *15*, 7505–7511. [CrossRef] [PubMed]
14. Chen, S.; Dai, L.; Liu, J.; Gao, Y.; Liu, X.; Chen, Z.; Zhou, J.; Cao, C.; Han, P.; Kanahiraa, M. The visible transmittance and solar modulation ability of $VO_2$ flexible foils simultaneously improved by Ti doping: An optimization and first principle study. *Phys. Chem. Chem. Phys.* **2013**, *15*, 17537–17543. [CrossRef] [PubMed]
15. Zhou, M.; Bao, J.; Tao, M.; Zhu, R.; Lin, Y.; Xie, Y. Periodic porous thermochromic $VO_2$(M) films with enhanced visible transmittance. *Chem. Commun.* **2013**, *49*, 6021–6023. [CrossRef] [PubMed]
16. Xu, G.; Jin, P.; Tazawa, M.; Yoshimura, K. Optimization of antireflection coating for $VO_2$-based energy efficient window. *Sol. Energy Mater. Sol. Cells* **2004**, *83*, 29–37. [CrossRef]
17. Jin, P.; Xu, G.; Tazawa, M.; Yoshimura, K. Design, formation and characterization of a novel multifunctional window with $VO_2$ and $TiO_2$ coatings. *Appl. Phys. A* **2003**, *77*, 455–459.
18. Kusano, E.; Theil, J.A. Effects of microstructure and nonstoichiometry on electrical properties of vanadium dioxide films. *J. Vac. Sci. Technol. A* **1989**, *7*, 1314–1317. [CrossRef]
19. Griffiths, C.H.; Eastwood, H.K. Influence of stoichiometry on the metal-semiconductor transition in vanadium dioxide. *J. Appl. Phys.* **1974**, *45*, 2201–2206. [CrossRef]
20. Jin, S.B.; Lee, J.S.; Choi, Y.S.; Choi, I.S.; Han, J.G. High-rate deposition and mechanical properties of $SiO_x$ film at low temperature by plasma enhanced chemical vapor deposition with the dual frequencies ultra high frequency and high frequency. *Thin Sol. Films* **2011**, *519*, 6334–6338. [CrossRef]
21. Wang, N.; Liu, S.; Zeng, X.T.; Magdassi, S.; Long, Y. Mg/W-codoped vanadium dioxide thin films with enhanced visible transmittance and low phase transition temperature. *J. Mater. Chem. C* **2015**, *3*, 6771–6777. [CrossRef]
22. Li, J.; Dho, J. Anomalous optical switching and thermal hysteresis behaviors of $VO_2$ films on glass substrate. *Appl. Phys. Lett.* **2011**, *99*, 231909. [CrossRef]
23. Petrov, G.I.; Yakovlev, V.V.; Squier, J. Raman microscopy analysis of phase transformation mechanisms in vanadium dioxide. *Appl. Phys. Lett.* **2002**, *81*, 1023–1025. [CrossRef]
24. Donev, E.U.; Lopez, R.; Feldman, L.C.; Haglund, R.F. Confocal raman microscopy across the metal-insulator transition of single vanadium dioxide nanoparticles. *Nano Lett.* **2009**, *9*, 702–106. [CrossRef] [PubMed]
25. Vernardou, D.; Louloudakis, D.; Spanakis, E.; Katsarakis, N.; Koudoumas, E. Functional Properties of APCVD $VO_2$ Layers. *Int. J. Thin Films Sci. Technol.* **2015**, *4*, 187–191.
26. Du, J.; Gao, Y.; Luo, H.; Kang, L.; Zhang, Z.; Chen, Z.; Cao, C. Significant changes in phase-transition hysteresis for Ti-doped $VO_2$ films prepared by polymer-assisted deposition. *Sol. Energy Mater. Sol. Cells* **2010**, *95*, 469–475. [CrossRef]

27. Kim, E.; Jiang, Z.; No, K. Measurement and calculation of optical band gap of chromium aluminum oxide films. *Jpn. J. Appl. Phys.* **2000**, *39*, 4820–4825. [CrossRef]
28. Jiang, M.; Li, Y.; Li, S.; Zhou, H.; Cao, X.; Bao, S.; Gao, Y.; Luo, H.; Jin, P. Room temperature optical constants and band gap evolution of phase pure M1-$VO_2$ thin films deposited at different oxygen partial pressures by reactive magnetron sputtering. *J. Nanomater.* **2014**, *2014*, 183954. [CrossRef]

© 2016 by the authors; licensee MDPI, Basel, Switzerland. This article is an open access article distributed under the terms and conditions of the Creative Commons Attribution (CC-BY) license (http://creativecommons.org/licenses/by/4.0/).